



Liquid Phase Selective Oxidation of Aromatic Alcohols Employing Nanoparticles of Zirconia Supported on Nickel Manganese Oxide: Synthesis, Characterization and Catalytic Evaluation

SAAD ALABBAD, S.F. ADIL, ABDULRAHMAN ALWARTHAN and M. RAFIQ H. SIDDIQUI*

Department of Chemistry, College of Science, King Saud University, P.O. 2455, Riyadh 11451, Kingdom of Saudi Arabia

*Corresponding author: E-mail: rafiqs@ksu.edu.sa

(Received: 4 December 2012;

Accepted: 9 September 2013)

AJC-14082

Zirconia nanoparticles supported on nickel manganese mixed oxide were synthesized by co-precipitation method. The catalytic properties of these materials were investigated for the oxidation of benzyl alcohol using molecular oxygen as oxidant. It was observed that calcination temperature plays an important role in the process. The catalyst calcined at 400 °C showed the highest catalytic activity for the oxidation of benzyl alcohol. Molecular oxygen was found to be the most efficient oxidant in the catalytic performance of the synthesized catalyst.

Key Words: Zirconia nanoparticles, Nickel manganese mixed oxide, Benzyl alcohol, Oxidation catalyst.

INTRODUCTION

Oxidation of aromatic alcohols to corresponding aldehydes is an important area of research for scientist around the world as they play a significant role of building blocks for many organic compounds¹⁻³. A large number of heterogeneous catalyst have been reported in literature⁴⁻¹² with regard to the conversion of alcohols to aldehydes using noble metals such as Pt, Ru, Au, Pd and their derivatives using oxygen as an oxidant. Platinum-based catalysts can be easily poisoned which make them sensitive and hence can be used only in mild conditions while gold catalysts have also been reported for their high selectivity towards aldehydes¹³. Silica supported catalysts have been reported widely in literature^{14,15} for gas-phase oxidations of ethylene and for methanol oxidations.

Nickel-manganese combination has been known to chemists for a long time, owing to their use as major components in alloys¹⁶⁻¹⁸, high-energy and high-power electrode material for alkaline cells¹⁹, lithium ion batteries²⁰, fuel cells²¹ and super capacitors²². Nickel and manganese as catalyst have been reported in literature for their use in deprotonative arene dimerization²³, oxidation of many precursors such as cyclohexene²⁴, CO, hydrocarbons²⁵⁻²⁷, partial oxidation of methane²⁸, electro oxidation of methanol²⁹, oxidative degradation of volatile organic compounds³⁰ hydration of acrylonitrile³¹ and xylene to terphthalic acid³². In order to investigate the possible application of nickel manganese mixed oxide as oxidation catalyst for the conversion of benzyl alcohol to benzaldehyde, we have earlier reported the synthesis of the nickel manganese oxide supported gold nanoparticles³³.

Herein, we reported the synthesis of nano zirconia supported nickel-manganese mixed oxide as oxidation catalyst for aromatic alcohols, using benzyl alcohol as the model compound. The synthesized catalyst was characterized by SEM, TEM, EADX, XRD, BET and TGA. The catalyst was tested for various substituted benzyl alcohol and the conversion was monitored using gas chromatography.

EXPERIMENTAL

Preparation of zirconia supported on nickel manganese oxide by deposition method: 95 mL of 0.2 M solutions of nickel nitrate and manganese nitrate were mixed in a round bottomed flask. To it was added 10 mL of 0.2 M solution of zirconium nitrate solution. The resulting solution was heated to 80 °C, while stirring using a mechanical stirrer and 1 M solution of NaHCO₃ was added drop wise until the solution attained a pH 9. The solution was continued to stir at the same temperature for 3 h and then left on stirring over night at room temperature. The solution was filtered using a Buchner funnel under vacuum and dried at 70 °C overnight. The product obtained was characterized using SEM, TEM, EADX, XRD, BET and TGA. The resulting powder was then calcined at different temperatures and was evaluated for its oxidation activity using benzyl alcohol as starting material.

Preparation of zirconia supported on nickel manganese oxide by modified deposition method: In this method of preparation of catalyst is divided into two parts: (a) Hydrothermal synthesis of zirconia nanoparticles, (b) Zirconia supported on nickel manganese oxide using deposition method.

Hydrothermal synthesis of zirconia nanoparticles: It was carried out using zirconium oleate as starting material, which was synthesized by reacting zirconium nitrate and sodium oleate. The zirconium oleate was then transferred into a PARR autoclave along with Triton X-100 and triethylene glycol and heated at 180 °C, for 3 h. After the autoclave was cooled, the sample was transferred into a centrifuge tube and centrifuged several times washing it with acetone and water to get rid of the organic impurities and other water soluble impurities. The isolated particles were then calcined at 250 °C.

Deposition synthesis of zirconia supported on nickel manganese oxide: The stoichiometric amount of the synthesized zirconia nanoparticles were dispersed in 95 mL of 0.2 M solutions of nickel nitrate and manganese nitrate were mixed in a round bottomed flask. The resulting solution was heated to 80 °C, while stirring using a mechanical stirrer and 1 M solution of NaHCO₃ was added drop wise until the solution attained a pH 9. The solution was continued to stir at the same temperature for 3 h and then left on stirring over night at room temperature. The solution was filtered using a Buchner funnel under vacuum and dried at 70 °C overnight. The product obtained was characterized using SEM, TEM, EADX, XRD, BET and TGA. The resulting powder was then calcined at different temperatures and was evaluated for its oxidation activity using benzyl alcohol as starting material.

Catalyst characterization: Scanning electron microscopy (SEM), elemental analysis and energy dispersive X-Ray analysis (EDX) were carried out using Jeol SEM model JSM 6360A (Japan). This was used to determine the morphology of nanoparticles and its elemental composition. Transmission electron microscopy (TEM) was carried out using Jeol TEM model JEM-1101 (Japan), which was used to determine the shape and size of nanoparticles. Powder X-ray diffraction studies were carried out using Altima IV: Regaku X-ray diffractometer. Fourier Transform Infrared Spectroscopy (FT-IR) the infrared spectra were recorded as KBr pellets using a Perkin-Elmer 1000 FT-IR spectrophotometer. BET surface area was measured on a NOVA 4200e surface area & pore size analyzer. Thermogravimetric Analysis (TGA) was carried out using Perkin-Elmer Thermogravimetric Analyzer 7.

Catalyst testing: In a typical reaction run, 300 mg of catalyst was loaded in a glass flask pre-charged with 0.2 mL (2 mmol) benzyl alcohol with 10 mL toluene as solvent; the mixture was then heated to 100 °C with vigorous stirring. Oxygen was bubbled at a flow rate of 20 mL min⁻¹ into the mixture once the reaction temperature was attained. After reaction, the solid catalyst was separated by centrifugation and the liquid samples were analyzed by gas chromatography to evaluate the conversion of the desired product by (GC, 7890A) Agilent Technologies Inc, equipped with a flame ionization detector (FID) and a 19019S-001 HP-PONA column.

RESULTS AND DISCUSSION

The synthesized catalyst was characterized by electron microscopy to evaluate the morphology and particle size of the catalyst. The scanning electron microscopy of the synthesized catalyst X % Zr-NiMnO, where X = (1, 3 and 5) pre-calcined at 400 °C was carried out and the micrographs are

shown in Figs. 1 and 2. It suggest that the morphology of the synthesized catalysts is like a bunch of nano flowers. The 1 % Zr-NiMnO showed some nano-rods which were absent in the 3 % Zr-NiMnO. It was also interesting to find that the catalyst 5 % Zr-NiMnO synthesized by the modified deposition method had a very different morphology. It was found to be spherical in shape and regular in size. The stoichiometric amount of doping could be confirmed from the EDX analysis to be approximately near to the calculated value.

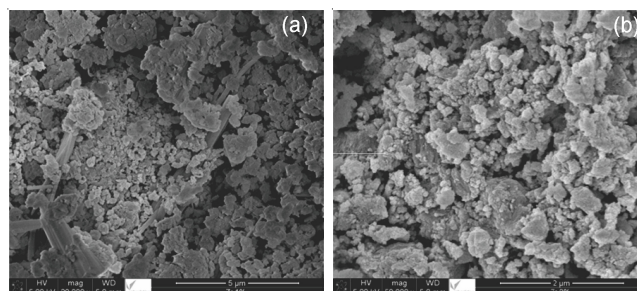


Fig. 1. SEM of the catalyst (a) 1 % Zr-NiMnO (b) 3 % Zr-NiMnO at 400 °C

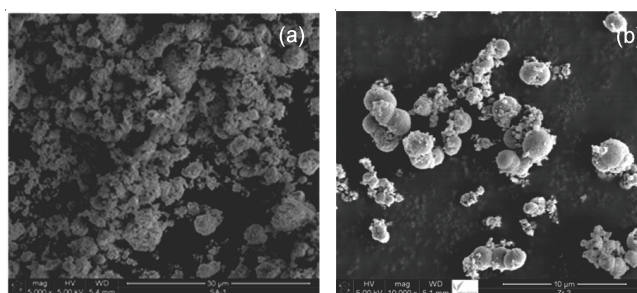


Fig. 2. SEM of the catalyst (a) 5 % Zr-NiMnO (b) 5 % Zr-NiMnO (modified) calcined at 400 °C

The TEM image of the catalyst 5 % Zr-NiMnO was carried out to know about the shape and size of the particles as shown in Fig. 3. The particle size distribution was calculated by using the general-purpose image processing program Image J software. It was found that the synthesized catalyst 1 % Zr-NiMnO possessed particle size of 0.61 nm, while 3 % Zr-NiMnO was found to contain particles of size 1.59 nm. When similar studies were carried out for 5 % Zr-NiMnO, calcined at 300, 400 and 500 °C, it was found that the particle size was found to be 3.53, 0.46, 0.43 nm, respectively. The particle size of the catalyst 5 % Zr-NiMnO synthesized by the modified synthetic procedure was found to be 0.69 nm.

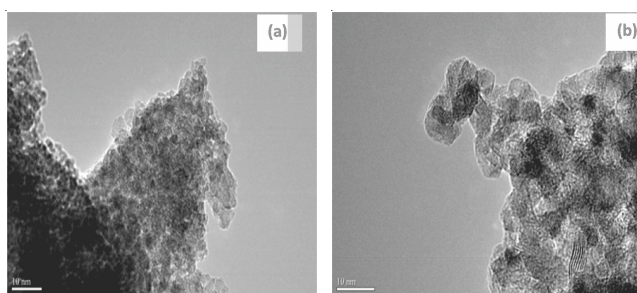


Fig. 3. TEM of the catalyst (a) 5 % Zr-NiMnO (400 °C) (b) 5 % Zr-NiMnO (500 °C)

Fig. 4 illustrates the X-ray diffraction pattern of 5 % Zr-NiMnO calcined at 300, 400 and 500 °C. The symbols in the Fig. 4 indicate the peaks of the corresponding phase.

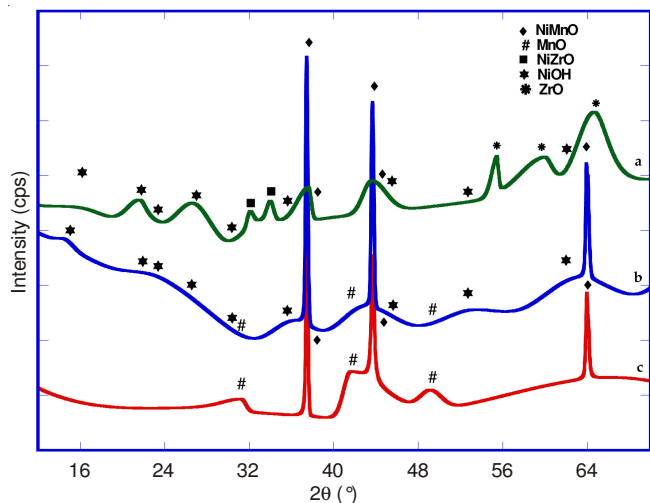


Fig. 4. XRD pattern of the synthesized 5 % Zr-NiMnO catalyst (a) 300 °C (b) 400 °C (c) 500 °C

Observations made in the XRD spectrum (Fig. 4) indicates that the catalyst 5 % Zr- NiMnO, calcined at 300 °C contains a mixture of cubic hexanickel manganese(IV) oxide (ICSD # 40584), orthorhombic β -manganese oxide (3/4) (ICSD # 40110) and orthorhombic dinickel dioxide hydroxide (ICSD # 202427). The catalyst calcined at 400 °C was found to contain peaks corresponding to a mixture of cubic hexa nickel manganese(IV) oxide (ICSD # 40584), orthorhombic dinickel dioxide hydroxide (ICSD # 202427) and a single peak of orthorhombic β -manganese oxide (3/4) (ICSD # 40110). The catalyst calcined at 500 °C was found to contain peaks corresponding to a mixture orthorhombic dinickel dioxide hydroxide with traces of cubic zirconium nickel oxide (4/2/1) (ICSD # 71964) and tetragonal zirconia (ICSD # 93028). When similar study of the XRD spectrum of X % Zr-NiMnO, where X = (1, 3 and 5) pre-calcined at 400 °C was carried out it was found that the 1 % Zr-NiMnO, 3 % Zr-NiMnO and 5 % Zr-NiMnO (modified) contains peaks corresponding to cubic hexanickel manganese(IV) oxide, while the spectrum of 5 % Zr-NiMnO contains mixture of cubic hexanickel manganese(IV) oxide and orthorhombic dinickel dioxide hydroxide. The presence of different phases of oxide along with the orthorhombic dinickel dioxide hydroxide may be attributed to the increase in catalytic activity of the catalyst 5 % Zr-NiMnO pre-calcined at 40 °C among the rest of the synthesized catalyst.

The synthesized catalyst was subjected to FT-IR spectroscopy and the spectrum was obtained (Fig. 5). From the % transmittance peaks in the region between 3450-3350 cm^{-1} characteristic of the OH group stretching vibration it can be concluded the presence of OH groups on the surface of the catalyst which may be due to the presence of moisture on the surface while the peak corresponding to OH in the IR spectrum of 5 % Zr-NiMnO catalyst could be due the presence of dinickel dioxide hydroxide which was established by observations of the XRD spectrum. While the peaks in the region 1600-1300 cm^{-1} are due to the metal/surface binding characteristics

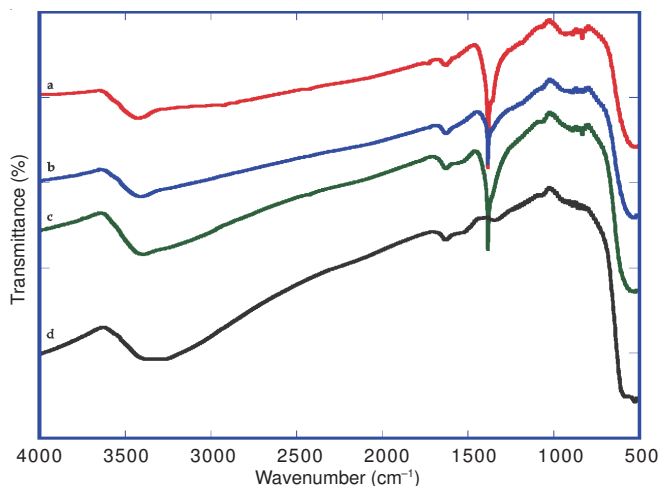


Fig. 5. FT-IR spectrum of the synthesized catalyst (a) 1 % Zr-NiMnO (b) 3 % Zr-NiMnO (c) 5 % Zr-NiMnO (d) 5 % Zr-NiMnO (modified)

possibly due to the metal-oxygen bond vibrations on the surface. The peaks in the region 700-550 cm^{-1} can be due to the stretching frequencies between the metal and oxygen atom.

The catalyst with different % loading of zirconia nanoparticles were subjected to TGA analysis to learn out about the thermal stability of the synthesized catalyst. Temperature was programmed from 25-1000 °C at a heating rate of 10 °C/min. It was observed that the almost all the synthesized catalyst is thermally stable, yielding a maximum loss of weight to be 16.4 % at 1000 °C found in the case 3 % zirconia nanoparticles loaded catalyst making it to be the least thermally stable among the synthesized catalyst, while the catalyst with 5 % Zr nanoparticles can be assumed to be the best thermally stable catalyst with a least weight loss % of just 7.6 % at 1000 °C. A graphical illustration is given in Fig. 6.

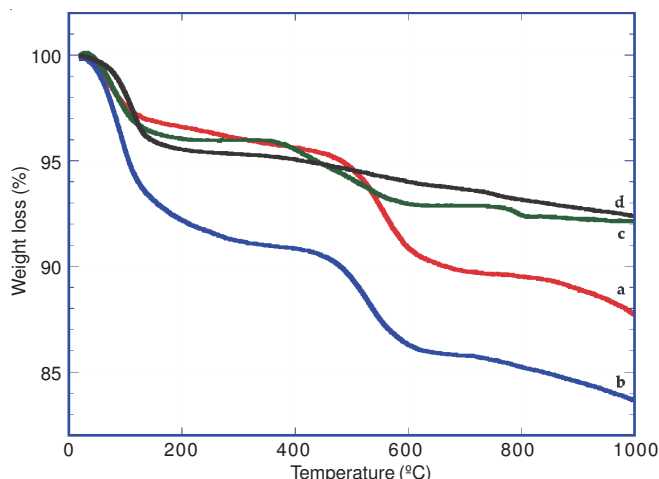


Fig. 6. TGA curves of the synthesized catalyst (a) 1 % Zr-NiMnO (b) 3 % Zr-NiMnO (c) 5 % Zr-NiMnO (d) 5 % Zr-NiMnO (modified)

In order to optimize the percentage of zirconia nanoparticles to be supported on the nickel-manganese mixed oxide for the best catalytic performance as oxidation catalyst, a series of catalyst with varying percentage of zirconia nanoparticles were synthesized and evaluated for their catalytic property using the oxidation of benzyl alcohol to benzaldehyde as a model reaction. The reaction was carried out at 100 °C, while passing

O₂ gas as a source of molecular oxygen. During the study it was found that the 1 % zirconia doped nickel manganese mixed oxide (1 % Zr-NiMnO) yielded a conversion of 70 %, while the catalyst with 3% zirconia doped nickel manganese mixed oxide (3 % Zr-NiMnO) yielded 67 %. A 100 % conversion of benzyl alcohol to benzaldehyde was obtained with the catalyst containing 5 % zirconia doped nickel manganese mixed oxide (5 % Zr-NiMnO). The selectivity in all the above reactions was found to be >99 %. In order to evaluate the effect of synthetic procedure on the catalytic performance of the synthesized catalyst, the catalyst synthesized with modified deposition method was used for the conversion and the conversion product obtained was 56 % and since the result obtained is not comparable as the rest, this method of synthesis was not employed further in the synthesis of catalysts. The results have been summarized in Table-1. A graphical illustration is given in Fig. 7.

Entry	Zr (%)	Conversion (%)
1	0	48
2	1	71.21
3	3	67.35
4	5	100
5	5 (Modi)	56

Reaction conditions: Amount of catalyst 300 mg; calcination temperature 400 °C; reaction temperature 100 °C; oxygen flow rate 20 mL min⁻¹; benzyl alcohol 2 mmol; toluene 10 mL; reaction time 2 h.

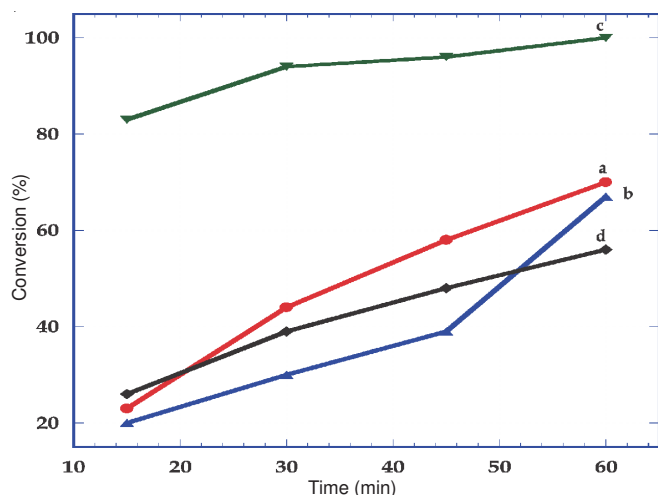


Fig. 7. Graphical illustration of the conversion of benzyl alcohol to benzaldehyde using of the synthesized catalyst (a) 1 % Zr-NiMnO (b) 3 % Zr-NiMnO (c) 5 % Zr-NiMnO (d) 5 % Zr-NiMnO (modified)

When the similar conversion was carried out to ascertain the optimum calcination temperature for the best catalytic performance of the synthesized catalyst, the 5 % Zr: NiMnO catalyst was calcined at different temperatures *i.e.*, 300, 400 and 500 °C. All the catalysts was subjected to the conversion of benzyl alcohol to benzaldehyde while maintaining similar reaction conditions as mentioned above. It was observed that the catalyst calcined at 300 °C the reaction starts off by yielding a 40 % conversion product after a time of 0.5 h and when the reaction was continued for another 150 min the conversion product obtained was 70 %, while in the case of 400 °C calcined catalyst the reaction starts off with 94 % conversion after 0.5 h and reaction is complete at 1 h with 100 % conversion product. When the 500 °C calcined catalyst was used a 51 % conversion product was obtained after 0.5 h of reaction time, while 81 % conversion was obtained at the end of 3 h of reaction time. The results are summarized in Table-2 and a graphical illustration is given in Fig. 8.

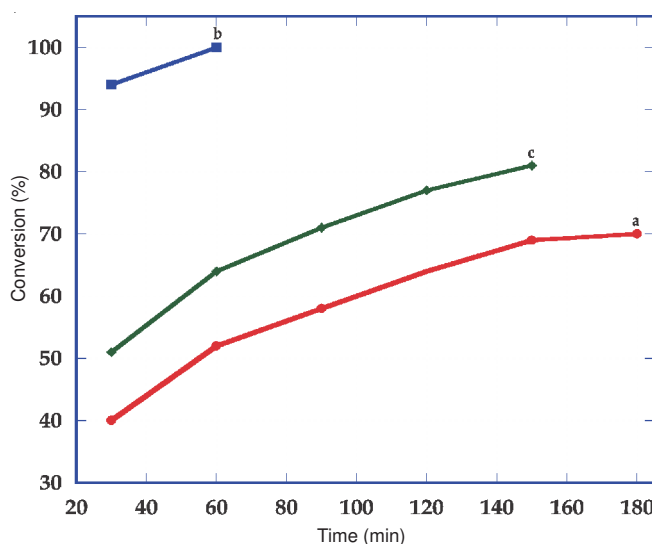


Fig. 8. Graphical illustration of the conversion of benzyl alcohol to benzaldehyde using of the synthesized catalyst 5 % Zr: NiMnO calcined at different temperatures (a) 300 °C (b) 400 °C (c) 500 °C

In order to check the compatibility and the effect of source of oxygen on catalytic performance of the synthesized catalyst 5 % Zr-NiMnO calcined at 400 °C, a few other sources of oxygen reported for similar conversion were employed and it was found that the catalyst displayed excellent performance with 100 % conversion and >99 % selectivity when molecular oxygen is used, when dibenzoyl peroxide and hydrogen peroxide were used 20 and 7 % conversion product was obtained, respectively. A graphical illustration is given in Fig. 9. The results have been summarized in Table-3.

Entry	Catalyst	Temperature (°C)	SA (m ² g ⁻¹)	Conversion (%)	Selectivity (%)
1	NiMnO	400	–	48.00	>99
2	5 % Zr-NiMnO	300	143.723	52.67	>99
3	5 % Zr-NiMnO	400	57.008	100.00	>99
4	5 % Zr-NiMnO	500	148.329	64.32	>99

Reaction conditions: Amount of catalyst 300 mg; reaction temperature 100 °C; oxygen flow rate 20 mL min⁻¹; benzyl alcohol 2 mmol; toluene 10 mL; reaction time 2 h.

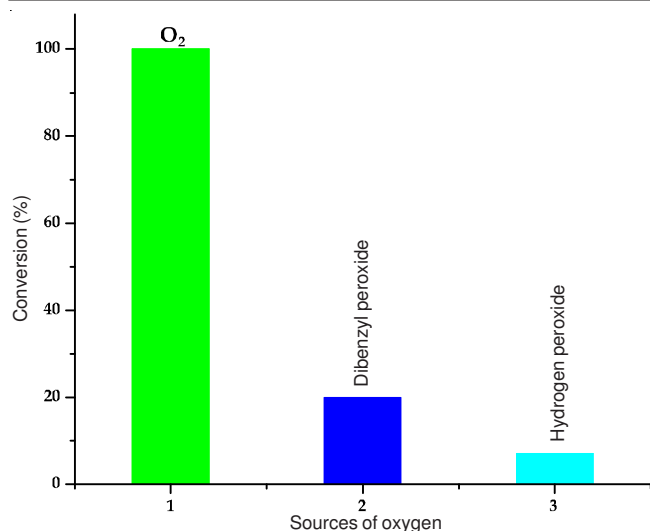


Fig. 9. Graphical illustration of the conversion of benzyl alcohol to benzaldehyde using of the synthesized catalyst 5 % Zr: NiMnO using different sources of oxygen

Entry	Oxidant	Conversion (%)
1	O ₂	100
2	Dibenzyl peroxide	20
3	Hydrogen peroxide	7

Reaction conditions: Amount of catalyst 300 mg; reaction temperature 100 °C; benzyl alcohol 2 mmol; toluene 10 mL; reaction time 2 h.

In order to understand the effect of catalyst on the solvent used, which is toluene in the present study, a blank reaction was carried out without the substrate benzyl alcohol using 5 % Zr-NiMnO as catalyst and no product was formation was observed. Hence it can be concluded that the conversion product benzaldehyde obtained is from the catalytic conversion of benzyl alcohol and not from toluene.

From the conversion of benzyl alcohol to benzaldehyde which was used as a model reaction it was ascertained that the best catalytic activity was displayed by 5 % Zr: NiMnO, calcined at 400 °C, which was established by spectral studies to contain mixture of cubic hexanickel manganese (IV) oxide and orthorhombic dinickel dioxide hydroxide. It can be concluded that the presence of orthorhombic dinickel dioxide hydroxide on the surface of the catalyst plays a crucial role. It was also found that the catalyst 5 % Zr: NiMnO (400 °C) possess least surface area according to the BET surface area analysis results, but yet has displayed best catalytic performance among the synthesized catalyst which could be due to the absence of orthorhombic dinickel dioxide hydroxide on the surface. As all the other catalyst synthesized were found to possess other phases of nickel manganese salts, which could not produce comparable catalytic performance. It was also confirmed that the catalyst performs best in the presence of molecular oxygen as source of oxygen. In order to determine the catalytic performance of 5 % Zr: NiMnO (400 °C), the reaction was carried out under similar conditions using a series of substituted benzyl alcohols, containing, 4-CH₃, 4-OCH₃, 4-Cl, 4-NO₂, 4-C(CH₃)₃, 4-CF₃ and 3-NO₂ groups as different substrates and their conversion to corresponding aldehydes

was studied. It was found that conversion product obtained was > 60 % and selectivity displayed by the catalyst was > 99 %. The results have been summarized in Table-4.

R. No.	Reactants	Products	Conversion (%)	Selectivity (%)
1			100	>99
2			63	>99
3			100	>99
4			100	>99
5			100	>99
6			65.12	>99
7			95	>99
8			100	>99

Reaction conditions: Catalyst 5 % Zr: NiMnO (400 °C); Amount of catalyst 300 mg; reaction temperature 100 °C; benzyl alcohol 2 mmol; toluene 10 mL; reaction time 2 h.

Conclusion

Nano zirconia supported nickel manganese oxide show high activity and stability for the oxidation of benzyl alcohol using molecular oxygen as a source of oxygen. A synergistic

effect between calcination temperatures and the chemical kinetics of the reaction was observed and it was confirmed that calcination temperature plays an important role forming an active and durable catalyst. It was noticed that molecular oxygen has substantial influence on the catalytic performance of the synthesized catalyst. It can be believed that this catalyst can be further used for the evaluation of its oxidative property for the synthesis of other important aromatic and aliphatic aldehydes can be explored.

ACKNOWLEDGEMENTS

This project was supported by King Saud University, Deanship of Scientific Research, College of Science, Research Center.

REFERENCES

- W.F. Hoelderich, *Catal. Today*, **62**, 115 (2000).
- R.A. Sheldon, I. Arends, G.J. Ten Brink and A. Dijkstra, *Acc. Chem. Res.*, **35**, 774 (2002).
- T. Mallat and A. Baiker, *Chem. Rev.*, **104**, 3037 (2004).
- T. Mallat, Z. Bodnar, A. Baiker, O. Greis, H. Strubig and A. Reller, *J. Catal.*, **142**, 237 (1993).
- Z. Opre, J.-D. Grunwaldt, M. Maciejewski, D. Ferri, T. Mallat and A. Baiker, *J. Catal.*, **230**, 406 (2005).
- M. Caravati, J.-D. Grunwaldt and A. Baiker, *Catal. Today*, **91-92**, 1 (2005).
- D.I. Enache, J.K. Edwards, P. Landon, B. Solsona-Espriu, A.F. Carley, A.A. Herzing, M. Watanabe, C.J. Kiely, D.W. Knight and G.J. Hutchings, *Science*, **311**, 362 (2006).
- H. Miyamura, R. Matsubara, Y. Miyazaki and S. Kobayashi, *Angew. Chem. Int. Ed.*, **46**, 4151 (2007).
- P. Haider, B. Kimmerle, F. Krumeich, W. Kleist, J.-D. Grunwaldt and A. Baiker, *Catal. Lett.*, **125**, 169 (2008).
- A. Abad, P. Concepcion, A. Corma and H. Garcia, *Angew. Chem. Int. Ed.*, **44**, 4066 (2005).
- S. Marx and A. Baiker, *J. Phys. Chem. C*, **113**, 6191 (2009).
- N. Dimitratos, J.A. Lopez-Sanchez, D. Morgan, A.F. Carley, R. Tiruvalam, C. J. Kiely, D. Bethell and G.J. Hutchings, *Phys. Chem. Chem. Phys.*, **11**, 5142 (2009).
- C. Della Pina, E. Falletta, L. Prati and M. Rossi, *Chem. Soc. Rev.*, **37**, 2077 (2008).
- X.E. Verykios, F.P. Stein and R.W. Coughlin, *Cat. Rev. Sci. Eng.*, **22**, 197 (1980).
- K. Ravi Kumar, P.V.V. Satyanarayana and B.S. Reddy, *Asian J. Chem.*, **24**, 3876 (2012).
- T.J. Williams, *Int. J. Pres. Ves. Pip.*, **81**, 657 (2004).
- J.-Y. Kim, C.-N. Park, J.-S. Shim, C.-J. Park, J. Choi, H. Noh, *J. Power Sources*, **180**, 648 (2008).
- R. Fathi, S. Sanjabi and N. Bayat, *Mater. Lett.*, **66**, 346 (2012).
- D. Kim, S.-H. Kang, M. Balasubramanian and C.S. Johnson, *Electrochem. Commun.*, **12**, 1618 (2010).
- S. Patoux, L. Sannier, H. Lignier, Y. Reynier, C. Bourbon, S. Jouanneau, F. Lecras and S. Martinet, *Electrochim. Acta*, **53**, 4137 (2008).
- V.S. Purnakala and J.B. Fernandes, *J. Power Sources*, **79**, 114 (1999).
- D.-L. Fang, Z.-D. Chen, B.-C. Wu, Y. Yan and C.-H. Zheng, *Mater. Chem. Phys.*, **128**, 311 (2011).
- T. Truong, J. Alvarado, L. D. Tran and O. Daugulis, *Org. Lett.*, **12**, 1200 (2010).
- M. Salavati-Niasar, *J. Mol. Catal. A*, **283**, 120 (2008).
- J.J. Spivey, In eds.: G.C. Bond and G. Webb, Complete Catalytic Oxidation of Volatile Organics, Catalysis, The Royal Society of Chemistry, Cambridge, Vol. 8 (1989).
- K.M. Parida and A. Samal, *Appl. Catal. A*, **182**, 249 (1999).
- C. Lahousse, A. Bernier, P. Grange, B. Delmon, P. Papaefthimiou, T. Ionnides and X. Verykios, *J. Catal.*, **178**, 1 (1998).
- M. Hadj-Sadok Ouaguenouni, A. Benadda, A. Kiennemann and A. Barama, *Compt. Rend. Chim.*, **12**, 740 (2009).
- I. Danaee, M. Jafarian, A. Mirzapoor, F. Gopal and M.G. Mahjani, *Electrochim. Acta*, **55**, 2093 (2010).
- S.A. Hosseini, A. Niaei, D. Salari and S.R. Nabavi, *Ceram. Int.*, **38**, 1655 (2012).
- A. Onda, S. Hara, K. Kajiyoshi and K. Yanagisawa, *Appl. Catal. A*, **321**, 71 (2007).
- G.G. Lavoie, Eastman Chemical Company, Patent Cooperation Treaty Application, WO05108340 (2005), European Patent Application, EP1756031 (2007).
- M.R.H. Siddiqui, S.F. Adil, R.M. Mahfouz and A. Al-Arifi, *Oxid. Commun.*, **35**, 476 (2012).